

Low noise surface mapping of transparent plane-parallel parts with a low coherence interferometer

Leslie L. Deck and Peter J. de Groot
Zygo Corporation, Laurel Brook Road, Middlefield, CT. USA, 06455-0448

ABSTRACT

A new instrument for measurements of thin transparent flats incorporates a novel in-line normal-incidence equal path interferometer, and extended broad-band illumination to isolate the surface of interest while reducing coherent noise and artifacts. Incorporating a 4Mpix camera, matching high resolution imaging system and vibration robust design; the instrument satisfies the needs of current and future hard disk and pellicle metrology.

1. INTRODUCTION

Laser Fizeau interferometric profilers based on phase-shifting interferometry (PSI)¹ routinely measure surfaces with high precision. However, because of interference from the other parallel surface, these tools often have difficulty measuring transparent plane-parallel parts like the glass disks used in high density hard drives and the pellicles used for semiconductor lithography applications. To satisfy the precision and resolution requirements for current and future hard disk and glass pellicle manufacturers, we have developed a Flat Glass Tester (FGT) based on a novel low coherence equal-path interferometer.^{2,3} This new instrument operates at 455nm for enhanced vertical resolution with respect to traditional HeNe based interferometers, and uses a 4Mpix camera (2048x2048 pixel) camera with matching optics for high lateral resolution. In addition to solving the problem of separating parallel semi-transparent reflecting surfaces, the FGT has extraordinarily low coherent noise and high overall performance with respect to alternative solutions, particularly for mid-spatial frequency measurements.

2. OPTICAL SYSTEM

Figure 1 shows the optical design of the FGT. The source is a high brightness LED with a mean wavelength of 455 nm and a removable 2-nm bandwidth interference filter. An optical relay sets the illumination cone angle to uniformly fill the 100mm instrument aperture and images the LED to fill the pupil conjugate at the aperture stop.

The interferometer cavity comprises an in-line high-quality flat beamsplitter and reference element and the object to be measured. The beamsplitter and reference are rigidly coupled and move together to perform the phase shifting. The first surface of the beamsplitter and the back surface of the reference are coated to produce high interference contrast across a wide variety of test surface reflectivities. The object surface is normal to the optical axis and at a position such that the optical path between the reference and beamsplitter equals the optical path between the beamsplitter and object. The interferometer components are tilted so that unwanted reflections from the illumination beam are stopped at the aperture. The result is high-contrast interference with fully incoherent illumination and low background light.

The use of low coherence illumination means that high contrast interference occurs over a limited range of test surface positions within $\pm 40 \mu\text{m}$ about the equal path condition (when the distance between the beamsplitter and test surfaces equals the distance between the beamsplitter and reference surfaces). This is the fundamental mechanism for separating the reflections from parallel surfaces of partially-transparent flat parts. Figure 2 shows a commercial implementation of this technology.

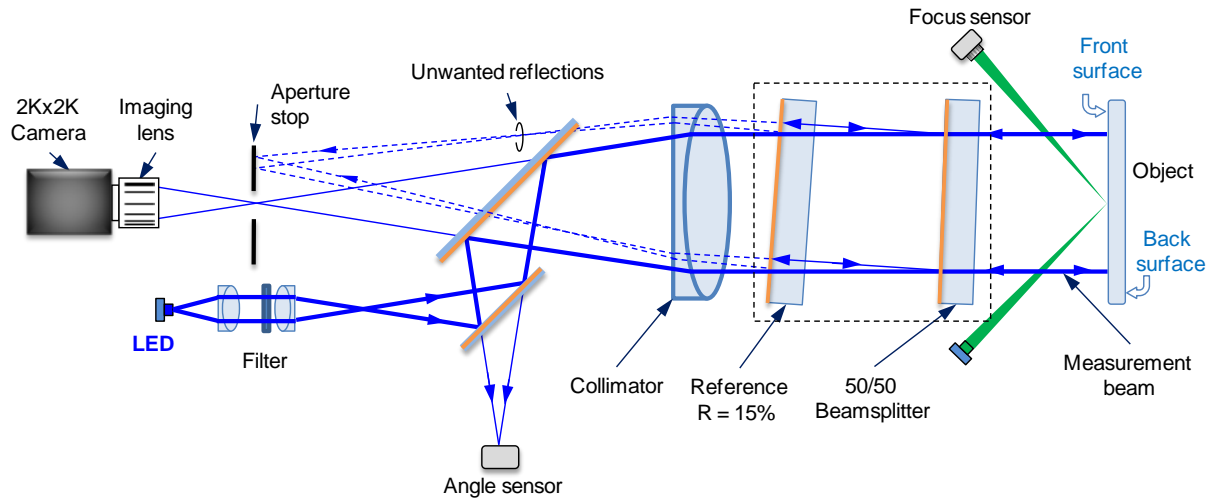


Figure 1: Basic optical layout. A broad-band extended source illuminates an interferometer cavity consisting of the 1st surfaces of the reference and beam-splitter elements and the object. Aided by the angle and focus sensor, the object surface is placed at the equal-path location (camera focus). Phase shifting is accomplished by moving the boxed elements as a whole.

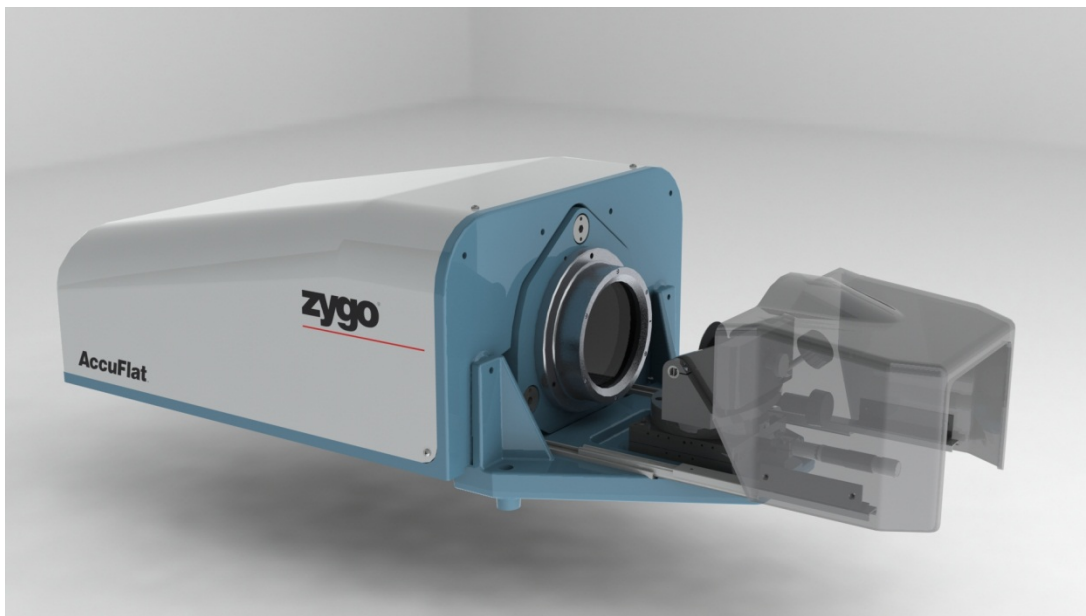


Figure 2: AccuFlat™ instrument based on the geometry of Figure 1. A retractable gray shield to control turbulence can be seen on the right which covers the part of the test cavity exposed to the air.

3. ALIGNMENT AIDS

For highest interference contrast and best performance, the test surface is aligned both parallel to the reference surface and set to the zero optical path difference (OPD). This alignment is facilitated with the two alignment aids shown in Figure 1. The user first adjusts the part tip and tilt by overlapping two reflected source images detected by the angle sensor—one from the reference surface and the other from the surface under test. Next the user moves the test surface to the plane of highest contrast with the aid of a triangulation focus sensor that continuously reports the distance of the object from the ideal, zero OPD position. The focus sensor also allows the user to identify and distinguish between the

front and back reflections from a transparent flat. The focus sensor has a range of $\pm 5\text{mm}$ along the optical axis and a resolution of $1\mu\text{m}$.

4. VIBRATION ROBUSTNESS

Vibration robustness is essential when measuring thin transparent parts, which are held gently to minimize surface distortion but are consequently sensitive to external vibrations. The FGT hardware and software were designed to be robust against vibrationally induced phase errors.⁴ Traditional PSI instruments are sensitive to particular vibrational frequencies that can generate cyclic errors that manifest themselves as periodic surface distortions, called ripple, at twice the fringe spatial frequency.⁵ The FGT reduces ripple errors from rigid-body vibrations by over an order of magnitude. Figure 3 shows the vibration frequency-amplitude product limit to achieve less than 1nm rms surface error compared to a conventional PSI instrument using a 5 frame phase shifting algorithm.⁶ Camera shuttering reduces contrast loss so that each acquired frame a “snapshot” of the interference pattern at an integration time of less than 1ms. The retractable shield shown in Figure 2 minimizes the residual effects of air turbulence.

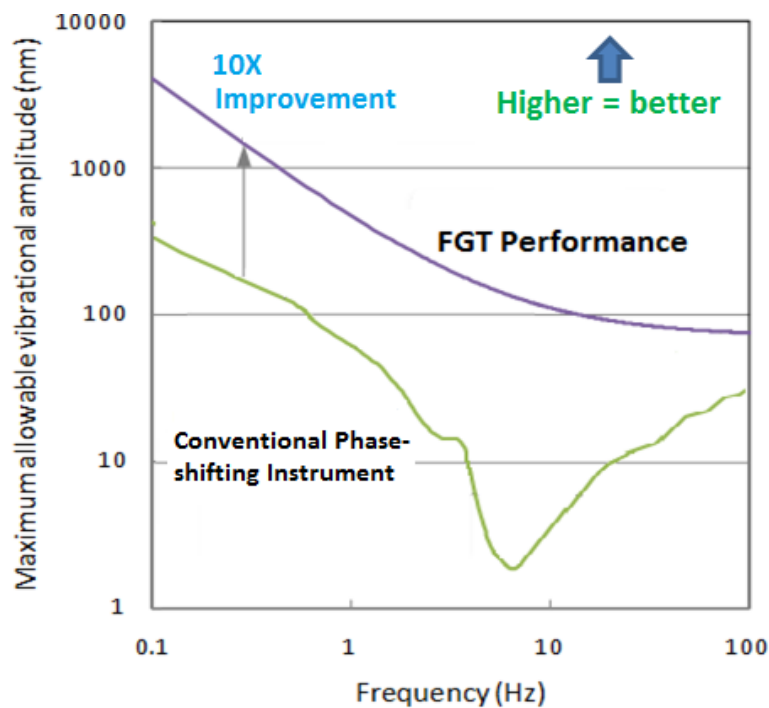


Figure 3: Maximum allowed vibration amplitude spectrum to achieve $<1\text{nm}$ rms ripple error for to the FGT compared to a conventional PSI instrument using a 5-bucket (5B) phase analysis. . A 10X improvement over conventional methods is realized over most of the frequency range relevant to production metrology.

5. PERFORMANCE

This combined low spatial and temporal coherence eliminates coherent artifacts and significantly reduces the effects of dust and particulates in the optical system, allowing the tool to meet very low noise specifications. An indication of the system measurement uncertainty can be derived from the uncertainty matrix⁷ which reports the standard deviation of each pixel from an ensemble of low order form subtracted measurements. Low order form is removed to minimize turbulence influences by using a 5mm period cutoff. Ideally the map of standard deviations should be uniform and Figure 4 shows this to be the case, predicting a 120pm single measurement rms repeatability with a standard deviation of 17pm.

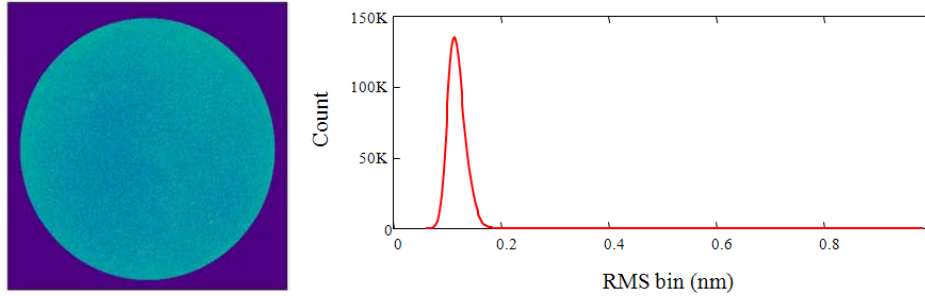


Figure 4: The left figure is the uncertainty matrix (the map of the standard deviations for each pixel) calculated from an ensemble of 50 measurements. The right figure shows the histogram of the standard deviations.

An important goal for the FGT is accurate measurements of surface mid- to high-spatial frequencies. To that end, the collimator and imaging lens are custom broad-band fixed-focus designs that produce less than 0.1% distortion across the 100mm field. Figure 5 shows the distortion performance of the optical system as predicted by ZEMAX, this was verified by measuring the centers of circular features in a specially fabricated distortion artifact.

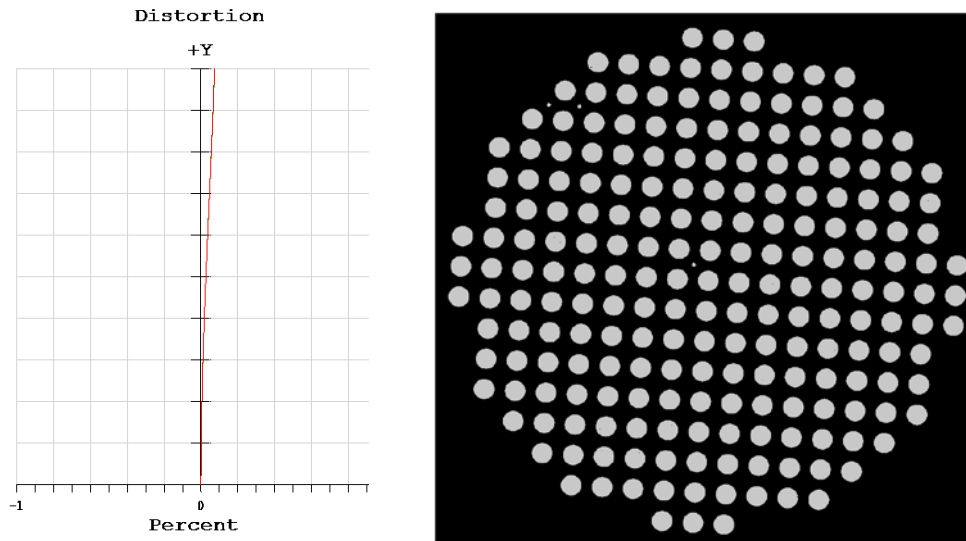


Figure 5: Distortion of the optical system as predicted by ZEMAX and verified by measuring the centers of circular features in a distortion measurement artifact (right).

Another goal was to measure surface structures with 200 micron periods (half Nyquist) with a transfer function of 70% and structures with 100 micron periods (Nyquist) at 40%. By design, the high interference contrast plane coincides with the plane of best focus for the high-quality imaging ocular. The ocular transfers this interference image onto a 4Mpix camera with effectively 50 μm sampling in object space. Measurements of the instrument transfer function with a small amplitude step artifact^{8,9} show a transfer function very close to these goals over most of the field (Figure 6). The high spatial frequency fidelity allows the instrument to detect small surface features including surface contaminants.

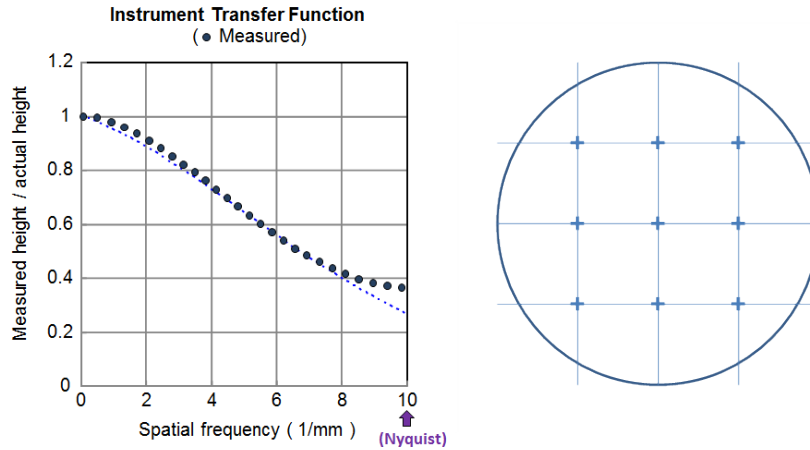


Figure 6: Measured system ITF (dots on left figure) as determined with a step artifact by averaging the ITF from 9 field locations indicated on right. Each field location produced the same ITF.

An additional consideration for accurately reproducing mid- to high-frequency surface features is a low coherent noise, achieved in the FGT by the use of a broad-bandwidth, extended LED light source in place of the highly coherent laser of conventional Fizeau interferometers. To isolate and quantify the residual coherent noise we measured the speckle decorrelation as a function of surface tilt.¹⁰ Figure 7 illustrates this decorrelation in the FGT by plotting the rms difference between a null measurement and measurements with various amounts of tilt. Each measurement in the plot represents 10 averages and is high pass filtered with a 1mm^{-1} spatial frequency to remove the effects of retrace and turbulence. The curve for a standard laser Fizeau instrument is included for comparison, illustrating a 3X to 5X improvement in rms noise for all values of tilt.

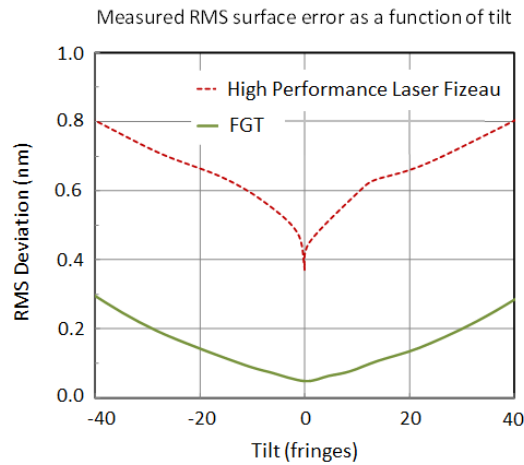


Figure 7: RMS residuals as a function of part tilt for the FGT compared to a standard laser Fizeau after high pass filtering to minimize turbulence affects. The FGT shows between a 3X to 5X lower noise.

As the local slope of the test surface departs from normal, the returning beams will follow different, non-common paths back to the imager. These divergent paths result in the accumulation of small phase differences which give rise to surface measurement error – also known as retrace error. Retrace error is estimated by measuring surface shape changes as a function of the relative tilt between the test and reference surface. This error manifests itself with specific spatial features, well described by Zernike polynomials. For the FGT optical system, there are four low order Zernike polynomials that dominate the distortion produced by retrace error, these are X and Y astigmatism (Zernike polynomials number 4 and 5)

and X and Y coma (polynomials 6 and 7) - both grow linearly with tilt. Figure 8 shows the dependence of both the astigmatism and coma magnitudes as a function of test surface tilt. Note that the upper tilt limit of 1mrad is extremely high, corresponding to 434 fringes across the field, and unlikely to occur in practice.

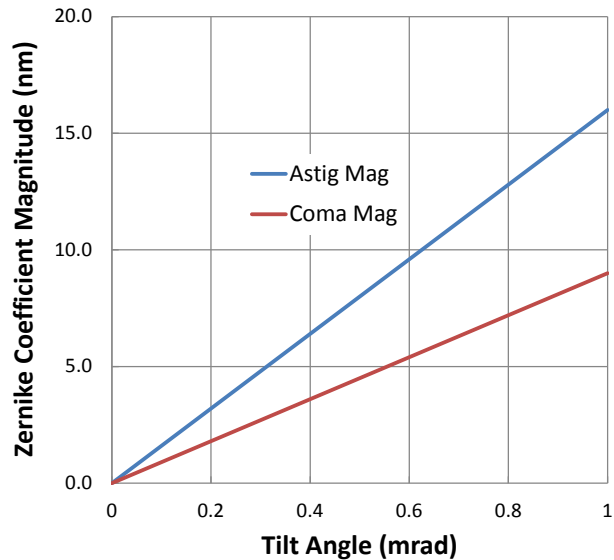


Figure 8: Measured Zernike astigmatism and coma magnitude coefficients as a function of test surface tilt.

6. EXAMPLE MEASUREMENTS

The instrument has been applied to the measurement of a variety of flat objects. Figure 9 shows measurements of both glass (4% reflectivity) and aluminum (80% reflectivity) hard disk blanks. The reference reflectivity of 15% assures that the interference contrast for these disk materials is better than 75% in spite of the large difference in surface reflectivity.

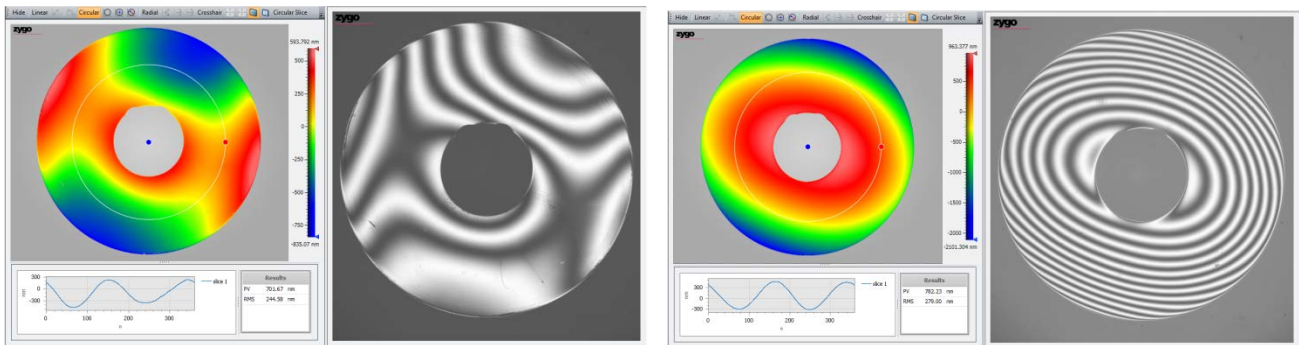


Figure 9: Measurements of 65mm hard disk blanks made of aluminum (left) and glass (right).

An industry standard method for assessing measurement precision is Gauge Repeatability and Reproducibility (Gauge R&R or GR&R). A GR&R uses an analysis of variance model to assess the measurement precision of the system through the precision/tolerance ratio (P/T). A P/T ratio of 10% usually indicates the system can reliably determine whether a part meets the tolerance.

A GR&R test was applied to the measurement of hard disk blanks for three parameters of importance to the manufacture and operation of these disks: Form PV and Waviness PV. These parameters represent the Peak-Valley (PV) departure of

the disk surface in low and high spatial frequency bands respectively. The GR&R procedure consisted of measuring a sample base of 10 glass disks three times each by three different operators, and calculating the P/T as the R&R variation as a percentage of the tolerance. There was no measurement averaging for this test. The Excel worksheet summary for the Form PV calculation is in Figure 10. Each parameter used a similar worksheet and tolerance levels were 3 microns for Form PV and 300nm for Waviness PV. The instrument measured the three parameters with 3% and 5% P/T ratio respectively, indicating that the instrument is an excellent tool for measuring the surface characteristics of these hard drive blanks.

zygo		Measurement System/Gage Capability Calculation Worksheet										
Part Name Hard Drive Disk				Gage Name AccuFlat				Part No. 000				
Parameter Disk Flatness - PV				Gage No.				Measurement Unit µm				
Tolerance (Spread) 3.0				Gage Type				Zero Equals 0 µm				
Operator A				Operator B				Operator C				
Sample #	1st Trial	2nd Trial	3rd Trial	Range	1st Trial	2nd Trial	3rd Trial	Range	1st Trial	2nd Trial	3rd Trial	Range
1	1.836	1.858	1.861	0.025	1.859	1.850	1.859	0.010	1.919	1.931	1.918	0.012
2	3.360	3.358	3.349	0.011	3.354	3.375	3.345	0.030	3.357	3.343	3.370	0.027
3	0.838	0.857	0.843	0.019	0.842	0.862	0.831	0.030	0.867	0.884	0.857	0.027
4	3.451	3.484	3.492	0.041	3.469	3.480	3.469	0.012	3.562	3.419	3.419	0.143
5	1.798	1.775	1.787	0.023	1.790	1.763	1.767	0.027	1.852	1.762	1.765	0.091
6	1.196	1.253	1.248	0.057	1.211	1.244	1.221	0.033	1.242	1.201	1.232	0.042
7	3.128	3.166	3.147	0.038	3.154	3.157	3.150	0.007	3.144	3.144	3.141	0.003
8	5.781	5.765	5.790	0.025	5.774	5.786	5.783	0.012	5.783	5.788	5.786	0.005
9	3.460	3.466	3.458	0.008	3.441	3.443	3.466	0.025	3.455	3.447	3.469	0.022
10	2.525	2.528	2.521	0.007	2.530	2.497	2.505	0.033	2.513	2.504	2.498	0.014
Average	2.737	2.751	2.750	0.025	2.742	2.746	2.739	0.022	2.769	2.742	2.746	0.039
Average-A			2.7460	Average-B			2.7425	Average-C			2.7524	
Test for Control:												
UCL-R = D4 * Rbar =												
D4 = 3.27 for 2 trials or 2.58 for 3 trials, enter the appropriate D4 value.												
<div style="display: flex; justify-content: flex-end; align-items: center;"> <input style="width: 50px; border: 1px solid black; margin-right: 5px;" type="text" value="2.58"/> <div style="border: 1px solid black; padding: 2px; margin-right: 5px;">0.074</div> UCLA-R </div>												
If any of the range values exceed the UCLA-R value, the measurement or reading should be reviewed, repeated corrected, or discarded as appropriate, and the new average and ranges should be computed.												
Measurement System/Gage Capability Analysis												
Equipment Variation ("Repeatability") = K1 * Rbar =												
where: K1 = 4.56 for 2 trials or 3.05 for 3 trials, enter the appropriate K1 value:												
<div style="display: flex; justify-content: flex-end; align-items: center;"> <input style="width: 50px; border: 1px solid black; margin-right: 5px;" type="text" value="3.05"/> <div style="border: 1px solid black; padding: 2px; margin-right: 5px;">0.087</div> Repeatability </div>												
Operator Variation ("Reproducibility") = K2 * Xbar_diff.												
where K2=3.65 for 2 and 2.70 for 3 operators, enter the appropriate K2 value:												
<div style="display: flex; justify-content: flex-end; align-items: center;"> <input style="width: 50px; border: 1px solid black; margin-right: 5px;" type="text" value="2.70"/> <div style="border: 1px solid black; padding: 2px; margin-right: 5px;">0.027</div> Reproducibility </div>												
Total "Repeatability" and "Reproducibility" Variation (R&R) =												
(R&R = Square root of ((Repeatability * Repeatability) + (Reproducibility * Reproducibility))												
<div style="display: flex; justify-content: flex-end; align-items: center;"> <div style="border: 1px solid black; padding: 2px; margin-right: 5px;">0.091</div> </div>												
% R & R = (100[(R&R)/(Tolerance)])												
<div style="display: flex; justify-content: flex-end; align-items: center;"> <div style="border: 1px solid black; padding: 2px; margin-right: 5px;">3.04%</div> </div>												
Acceptability:												
An R&R of 10% or less is excellent; 11-20% is adequate; 21-30% is marginally acceptable; and more than 30% is unacceptable.												
A analysis by: <input style="width: 100px; border: 1px solid black;" type="text" value="Initials EM"/>												
Date: <input style="width: 100px; border: 1px solid black;" type="text" value="Date: 07.20.11"/>												

Figure 10: Worksheet for Form PV produced from the GR&R measurements.

The FGT's low noise combined with surface localization is very useful for measuring surfaces in the presence of strong unwanted reflections. One particularly difficult measurement with standard Fizeau interferometers is the front surface of a solid retro-reflector. As Figure 11 shows, the FGT easily separates and measures the front surface in a single measurement with no hint of errors from the large, unevenly-distributed background light generated by the retroreflection from the back faces of the object, even across the dark edges at the intersections of the three faces.

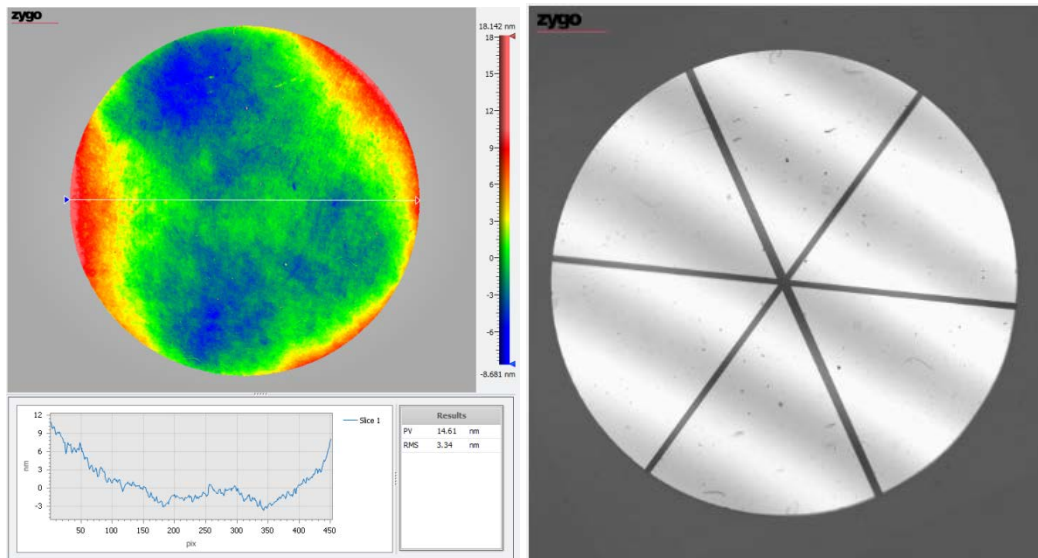


Figure 11: Single acquisition measurement of the front surface of a 1 inch solid glass retro. Note the low contrast fringes, yet the surface measurement shows neither artifacts nor fringe bleed through.

The short source coherence can separate surfaces for disks and pellicles as thin as 100 microns. Figure 12 shows substrate and top surface measurements of an 80% reflective mirror coated with 100 micron layer of fused silica. The fused silica top surface measurement is particularly difficult because of the loss in intensity dynamic range due to the large DC reflection from the mirrored surface, but the low noise characteristics of the FGT provides excellent surface measurement fidelity, even for low contrast surfaces. Of course, the substrate measurement will be influenced by the optical path variations through the film.

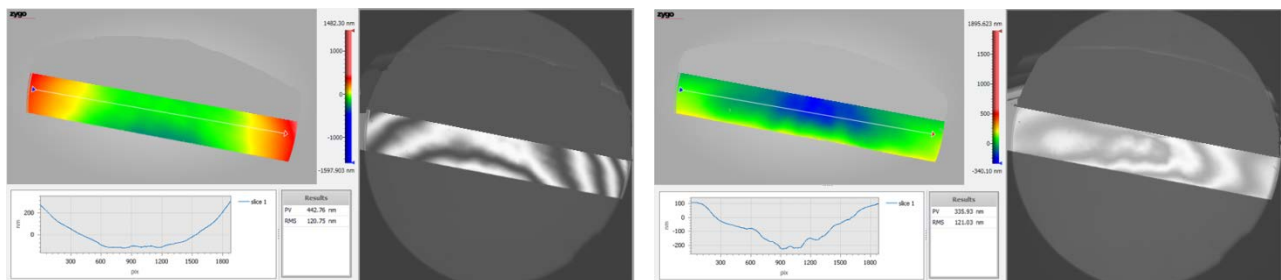


Figure 12: Measurement of the substrate (left) and top surface (right) of a mirror coated with a 100 micron thick fused silica layer.

7. CONCLUSIONS

The FGT is of interest as a metrology tool for thin transparent parts as well as for high resolution, low-noise measurements of all flat parts. The novel in-line, normal-incidence equal path interferometer geometry and extended broad-band illumination suppresses multiple-surface interference and reduces coherent noise and optical artifacts. System noise is typically 3X to 5X lower than a comparable laser Fizeau interferometer. The system also incorporates new phase analysis software to reduce vibration sensitivity and passive shields for turbulence mitigation. Incorporating a 4Mpix camera and a matching low-distortion, high resolution imaging system, the instrument combines 50 micron sampling resolution with excellent system transfer function characteristics. Though the design is intended to satisfy the needs of current and future hard disk and pellicle metrology, the instrument can be used to measure any flat surface with high

precision and without interference from other parallel surfaces, making it particularly useful for prisms and retroreflectors.

- 1 J. Greivenkamp and J. Bruning, Chap. 14, of "Optical Shop Testing", D. Malacara, ed. (J. Wiley, 1992)
- 2 P. de Groot, et al., published US Patent Application 20110007323 (2011). Additional U.S. and foreign patents pending.
- 3 L. Deck, P. de Groot, J. Soobitsky, "High precision interferometric testing of transparent, thin plane-parallel parts," Proc. SPIE Optifab, TD07-23 (2011)
- 4 US patents 7796273, 7796275, 7948639. Additional U.S. and foreign patents pending.
- 5 P. de Groot, "Vibration in phase shifting interferometry," Appl. Opt. 35, 6655-6662 (1996)
- 6 J. Schwider et. al., "Digital wave-front measuring interferometry: some systematic error sources," Appl. Opt. 22, 3421-3432 (1983)
- 7 C. Evans, "Uncertainty evaluation for measurements of peak-to-valley surface form errors," CIRP Annals 57, 509-512 (2008)
- 8 P. de Groot and X. Colonna de Lega, "Interpreting interferometric height measurements using the instrument transfer function " Proc. FRINGE 2005, W. Osten, Ed., 30-37 (Springer Verlag, Berlin Heidelberg, (2006).
- 9 P. Z. Takacs, E. L. Church, "A step-height standard for surface profiler calibration", Proc. SPIE 1995, 235 (1993)
- 10 K. Freischlad, "Interferometer for optical waviness and figure testing," Proc SPIE 3098, 53-61 (1997)